PLOS ONE

RESEARCH ARTICLE

Oncolytic virotherapy promotes radiosensitivity in soft tissue sarcoma by suppressing anti-apoptotic MCL1 expression

Toshinori Omori[1], Hiroshi Tazawa[2,3]*, Yasuaki Yamakawa[1], Shuhei Osaki[1], Joe Hasei[1], Kazuhisa Sugiu[1], Tadashi Komatsubara[1], Tomohiro Fujiwara[1], Aki Yoshida[1], Toshiyuki Kunisada[1,4], Yasuo Urata[5], Shunsuke Kagawa[2,6], Toshifumi Ozaki[1], Toshiyoshi Fujiwara[2]

1 Department of Orthopaedic Surgery, Okayama University Graduate School of Medicine, Dentistry and Pharmaceutical Sciences, Okayama, Japan, **2** Department of Gastroenterological Surgery, Okayama University Graduate School of Medicine, Dentistry and Pharmaceutical Sciences, Okayama, Japan, **3** Center for Innovative Clinical Medicine, Okayama University Hospital, Okayama, Japan, **4** Department of Medical Materials for Musculoskeletal Reconstruction, Okayama University Graduate School of Medicine, Dentistry and Pharmaceutical Sciences, Okayama, Japan, **5** Oncolys BioPharma, Inc., Tokyo, Japan, **6** Minimally Invasive Therapy Center, Okayama University Hospital, Okayama, Japan

* htazawa@md.okayama-u.ac.jp

Citation: Omori T, Tazawa H, Yamakawa Y, Osaki S, Hasei J, Sugiu K, et al. (2021) Oncolytic virotherapy promotes radiosensitivity in soft tissue sarcoma by suppressing anti-apoptotic MCL1 expression. PLoS ONE 16(4): e0250643. https://doi.org/10.1371/journal.pone.0250643

Editor: Ilya Ulasov, Sechenov First Medical University, RUSSIAN FEDERATION

Received: January 5, 2021

Accepted: April 8, 2021

Published: April 22, 2021

Data Availability Statement: All relevant data are within the paper and its supporting information files.

Funding: This study was supported in part by grants from the Ministry of Education, Science, and Culture, Japan (T. Fujiwara, Nos. 25293283 and 16H05416; T. Ozaki, No. 25293323; T. Kunisada, Nos. 25462333 and 16K10862; K. Sugiu, No. 15K10446; and H. Tazawa, No. 16K10596). Oncolys BioPharma, Inc. provided support in the form of salaries for Y. Urata, but did not have any

Abstract

Soft tissue sarcoma (STS) is a rare cancer that develops from soft tissues in any part of the body. Despite major advances in the treatment of STS, patients are often refractory to conventional radiotherapy, leading to poor prognosis. Enhancement of sensitivity to radiotherapy would therefore improve the clinical outcome of STS patients. We previously revealed that the tumor-specific, replication-competent oncolytic adenovirus OBP-301 kills human sarcoma cells. In this study, we investigated the radiosensitizing effect of OBP-301 in human STS cells. The *in vitro* antitumor effect of OBP-301 and ionizing radiation in monotherapy or combination therapy was assessed using highly radiosensitive (RD-ES and SK-ES-1) and moderately radiosensitive (HT1080 and NMS-2) STS cell lines. The expression of markers for apoptosis and DNA damage were evaluated in STS cells after treatment. The therapeutic potential of combination therapy was further analyzed using SK-ES-1 and HT1080 cells in subcutaneous xenograft tumor models. The combination of OBP-301 and ionizing radiation showed a synergistic antitumor effect in all human STS cell lines tested, including those that show different radiosensitivity. OBP-301 was found to enhance irradiation-induced apoptosis and DNA damage via suppression of anti-apoptotic myeloid cell leukemia 1 (MCL1), which was expressed at higher levels in moderately radiosensitive cell lines. The combination of OBP-301 and ionizing radiation showed a more profound antitumor effect compared to monotherapy in SK-ES-1 (highly radiosensitive) and HT1080 (moderately radiosensitive) subcutaneous xenograft tumors. OBP-301 is a promising antitumor reagent to improve the therapeutic potential of radiotherapy by increasing radiation-induced apoptosis in STS.

additional role in the study design, data collection and analysis, decision to publish, or preparation of the manuscript.

Competing interests: Y. Urata is President & CEO of Oncolys BioPharma, Inc., the manufacturer of OBP-301 (Telomelysin) and H. Tazawa and T. Fujiwara are consultants of Oncolys BioPharma, Inc.. This does not alter our adherence to PLOS ONE policies on sharing data and materials. The other authors have no potential conflicts of interest to disclose.

Introduction

Soft tissue sarcoma (STS) is a rare cancer that develops from the soft tissues of any part of the body. Sarcoma is the third most common cancer in children, accounting for 15.4% of malignant tumors of childhood, and 13,170 new cases of osteosarcoma and STS are diagnosed in the United States annually [1]. Treatment for STS requires a multidisciplinary approach that involves surgery, radiotherapy, and chemotherapy [2], with the standard approach for localized STS focusing on surgery and radiotherapy. Despite major advances in the treatment of STS however, poor response to radiotherapy is a critical prognostic factor, and radiotherapy-refractory patients often show tumor recurrence, distant metastasis and poor prognosis [3,4]. Therefore, the enhancement of sensitivity to radiotherapy is a critical aspect of improving the clinical outcome of STS patients.

Radiotherapy is used in STS patients for the local control of residual tumors after surgical resection [5]. However numerous complications, including fractures, fibrosis, edema, and contractures, hamper the efficacy of this approach. In addition, radiotherapy has the potential to cause secondary cancers in irradiated tissues [6]. Therefore, radiosensitizing approaches are required to reduce the dosage of ionizing radiation delivered to STS patients, especially in certain histological subtypes where the response to radiotherapy is known to be limited [7]. STS can be divided into distinct histological subtypes, including fibrosarcoma, leiomyosarcoma, rhabdomyosarcoma, Ewing sarcoma, myxosarcoma, peripheral nerve sheath tumor and perivascular wall tumor [8]. Ewing sarcoma is relatively sensitive to radiotherapy compared to other STS tumors, however, the precise mechanism determining sensitivity or resistance to radiotherapy in this disease remains unknown.

Although sensitivity to radiotherapy varies between the histological subtypes of STS, the underlying mechanism has not been clearly understood. Exposure of cells to ionizing radiation leads to a number of types of DNA damage, including DNA double-stranded breaks, which can be detected by the accumulation of γH2AX protein [9]. The expression level of γH2AX (H2AX phosphorylated at Ser139), is a strong biomarker of double-stranded DNA damage caused by ionizing radiation [9]. After its initial induction in irradiated tumor cells, the expression of γH2AX is gradually reduced by the activation of DNA damage repair [10]. In contrast, tumor cells possess an anti-apoptotic member of the B-cell lymphoma 2 (BCL2) family proteins, including BCL2, myeloid cell leukemia 1 (MCL1), and B-cell lymphoma-extra large (BCL-xL), to reduce radiation-induced apoptosis. Among the BCL2 family proteins, MCL1 is frequently overexpressed in various types of malignant tumor, including sarcoma [11]. Therefore, DNA damage repair and anti-apoptotic function may be involved in the radiosensitivity of STS.

As a novel therapeutic strategy for treating malignant tumors, we previously generated a telomerase-specific, replication-competent oncolytic adenovirus, OBP-301 (Telomelysin), in which the human telomerase reverse transcriptase (*hTERT*) promoter drives the expression of adenoviral *E1A* and *E1B* genes [12]. We confirmed the antitumor effect of monotherapy OBP-301 in epithelial and mesenchymal types of malignant tumor cells, including osteosarcoma and STS [12–14], as well as its use in combination with radiation [15] or chemotherapy [16–18]. A phase 1 clinical study of OBP-301 was conducted in the United States, with the safety of intratumoral injection of OBP-301 demonstrated in patients with a variety of advanced solid tumors, including sarcoma [19]. In combination with chemotherapy, we have shown that OBP-301 adenoviral E1A suppresses the expression of anti-apoptotic MCL1 protein, resulting in the enhancement of apoptosis induced by cisplatin and doxorubicin [17] or zoledronic acid [18]. Furthermore, in combination with radiotherapy, OBP-301 adenoviral E1B inhibits the repair machinery for DNA double strand breaks, enhancing radiation-induced apoptosis [15].

However, whether OBP-301 can enhance the sensitivity to radiotherapy in STS remains unclear.

In the present study, we investigated the radiosensitizing effect of OBP-301 in human STS cell lines. The *in vitro* efficacy of combined OBP-301 and ionizing radiation was assessed based on cell viability, apoptosis induction, and DNA damage status. In addition, we assessed the *in vivo* antitumor effect of the combination of OBP-301 and ionizing radiation using subcutaneous xenograft tumor models for two STS cell lines with different baseline radiosensitivities.

Materials and methods

Cell lines

We used four human STS cell lines, RD-ES (Ewing sarcoma), SK-ES-1 (Ewing sarcoma), HT1080 (fibrosarcoma), and NMS-2 (malignant peripheral nerve sheath tumor, MPNST) [20]. RD-ES, SK-ES-1, and HT1080 cells were obtained from the American Type Culture Collection (ATCC, Manassas, VA, USA). NMS-2 cells were kindly provided by Dr. Hiroyuki Kawashima (Niigata University, Niigata, Japan). Cells were not cultured for more than 5 months following thawing. The authentification was not performed by the authors. RD-ES and NMS-2 were grown in RPMI-1640 medium; SK-ES-1 cells were grown in McCoy's 5a medium; HT1080 cells were grown in Eagle's Minimum Essential Medium. All media were supplemented with 10% fetal bovine serum, 100 U/mL penicillin, and 100 μg/mL streptomycin. The cells were maintained at 37˚C in a humidified atmosphere with 5% CO_2.

Recombinant adenovirus

The recombinant telomerase-specific replication-competent adenovirus OBP-301 (Telomelysin), in which the *hTERT* promoter element drives the expression of the adenoviral *E1A* and *E1B* genes linked by an internal ribosome entry site, was previously constructed and characterized [12–14]. The particle and infectious titers of OBP-301 were 1×10^{12} viral particles (VP)/mL and 1×10^{11} plaque-forming units (PFU)/mL, respectively. The VP/PFU ratio of OBP-301 was 10.

Cell viability assay

RD-ES and SK-ES-1 cells were seeded at a density of 3×10^3 cells/well, and HT1080 and NMS-2 cells were seeded at a density of 1×10^3 cells/well on 96-well plates, 24 h before irradiation or OBP-301 infection. In monotherapy, cells were irradiated at dosages of 0, 1, 2, 5, or 10 Gy using an MBR-1520R irradiator (Hitachi Medical Co., Tokyo, Japan). In combination therapy, cells were infected with OBP-301 at multiplicity of infections (MOIs) of 0, 1, 5, 10, or 50 PFU/cell. Twenty-four hours after infection, cells were irradiated at dosages of 0, 1, 2, 5, or 10 Gy. Cell viability was determined on day 4 after irradiation using a Cell Proliferation Kit II (Roche Molecular Biochemicals Indianapolis, IN, USA) according to the manufacturer's protocol. The combined effect of OBP-301 and ionizing radiation was analyzed by calculating the combination index using the CalcuSyn software (BioSoft, Inc., Cambridge, UK). The computation of the combination index was based on the method of Chou [21].

Western blot analysis

SK-ES-1 and HT1080 cells (1×10^5 cells), seeded in a 100-mm dish, were prepared for protein extraction. Cells were treated with OBP-301 at the indicated MOIs for 48 h and/or were irradiated at the indicated dosages 24 h after infection. Cells were transfected with 10 nM MCL1

small interfering RNA (siRNA), or control siRNA (Applied Biosystems, Foster City, CA, USA) using Lipofectamine RNAiMAX (Invitrogen, Carlsbad, CA, USA) for 48 h and/or irradiated at the indicated dosages. Twenty-four hours after irradiation, whole cell lysates were prepared in a lysis buffer (50 mM Tris-HCl (pH 7.4), 150 mM NaCl, 1% Triton X-100) containing a protease inhibitor cocktail (Complete Mini; Roche Applied Science, Mannheim, Germany). To further assess DNA damage, SK-ES-1 cells (1×10^5 cells), seeded in a 100-mm dish, were infected with OBP-301 (10 MOI) and then irradiated at 1 Gy, 24 h after infection. Cells were harvested 0.5, 1, and 3 h after irradiation, and whole cell lysates were analyzed by Western blot for γH2AX expression.

Proteins (20 μg per lane) were separated on 8–15% sodium dodecyl sulfate polyacrylamide gels and transferred to polyvinylidene difluoride membranes (Hybond-P; GE Healthcare, Buckinghamshire, UK). Blots were blocked with Blocking-One (Nacalai Tesque, Kyoto, Japan) at room temperature for 30 min. The primary antibodies used were: mouse anti-Ad5 E1A monoclonal antibody (mAb) (554155; BD Bioscience, Franklin Lakes, NJ, USA); mouse anti-γH2AX mAb (05–636; Merck Millipore, Billerica, Massachusetts, USA); rabbit anti-poly (ADP-ribose) polymerase (PARP) polyclonal antibody (pAb) (9542), rabbit anti-MCL-1 mAb (39224), and rabbit anti-E2F1 mAb (3742; Cell Signaling Technology, Danvers, MA, USA); and mouse anti-β-actin mAb (A5441; Sigma-Aldrich, St. Louis, MO, USA). The secondary antibodies used were: horseradish peroxidase-conjugated antibodies against rabbit IgG (NA934; GE Healthcare) or mouse IgG (NA931; GE Healthcare). Immunoreactive protein bands were visualized using enhanced chemiluminescence (ECL Plus; GE Healthcare).

Immunofluorescence staining

SK-ES-1 cells, seeded on tissue culture chamber slides, were infected with OBP-301 (5 MOI) for 48 h. Cells were irradiated at 1 Gy, and then 30 min, 1 h, or 3 h following irradiation, cells were fixed with chilled 1% paraformaldehyde in phosphate-buffered saline (PBS) for 10 min on ice. The slides were subsequently incubated with primary mouse anti-γH2AX mAb (05–636; Millipore) for 24 h. After washing three times with PBS, slides were incubated with the secondary FITC-conjugated antibody against mouse IgG (61–6511; Zymed Laboratories Inc., South San Francisco, CA, USA) for 30 min on ice. The slides were further stained with ProLong® Gold antifade reagent with DAPI (life technologies Co., Carlsbad, CA, USA) and then analyzed under a confocal laser microscope (FV10i; Olympus Co., Tokyo, Japan).

In vivo subcutaneous human STS xenograft tumor models

Animal experimental protocols were approved by the Ethics Review Committee for Animal Experimentation of Okayama University School of Medicine. The experiments were conducted in accordance with the Policy on the Care and Use of the Laboratory Animals, Okayama University. All mice were maintained under barrier conditions with sterile diet and water. Under general anesthesia with 2% isoflurane, SK-ES-1 (5×10^6 cells/mouse) and HT1080 (3×10^6 cells/mouse) cells were subcutaneously inoculated into the flanks of 5- to 6-week-old female BALB/c *nu/nu* mice (CLEA Japan, Tokyo, Japan). When tumors reached 5 to 7 mm in diameter, the mice were irradiated at a dosage of 1 Gy/tumor (SK-ES-1) or 3 Gy/tumor (HT1080) every week for one or three cycles starting at day 0. During irradiation, mice were placed in a prone position, using custom-made holders that contain lead collimators to shield the upper half of the animal. A 50 μL solution containing OBP-301 at a dose of 1×10^8 PFU/tumor or PBS was injected into the tumors every week for one or three cycles. The perpendicular diameter of each tumor was measured every 3–4 days, and tumor volume was calculated with the following formula: tumor volume (mm^3) = $a \times b^2 \times 0.5$, where a is the longest

diameter, *b* is the shortest diameter, and 0.5 is a constant to calculate the volume of an ellipsoid. Animals were monitored every 3–4 days and there were no severe signs of illness or death due to the experimental procedures. When the mean tumor volume reached 4000 mm^3, mice were sacrificed by cervical dislocation after general anesthesia with 2% isoflurane.

Histopathologic analysis

Tumors were fixed in 10% neutralized formalin and embedded in paraffin blocks. Sections were stained with hematoxylin/eosin. Sections were also prepared for immunohistochemical examination using mouse anti-γH2AX mAb (05–636; Millipore) and rabbit anti-Ki67 mAb (ab16667; Abcam, Cambridge, UK). Immunoreactive signals were visualized using 3,3'-diaminobenzidine (DAB) solution (Nichirei Bioscience, Tokyo, Japan), and nuclei were counterstained with hematoxylin. All sections were analyzed under a light microscopy.

TUNEL staining

Sections were deparaffinized and put into 3% hydrogen peroxide for 10 min at room temperature. After nonspecific binding sites were blocked, the sections were incubated for 60 min at 37˚C with terminal deoxynucleotidyltransferase mediated dUTP nick end labeling (TUNEL; Roche Applied Science, Penzberg, Germany) and stained with DAB solution. Finally, all sections were counterstained with hematoxylin. Sections were rinsed with PBS after every step.

Statistical analysis

Data were expressed as mean ± SD. Differences between two groups were examined for statistical significance with the Student's *t* test. One-way ANOVA followed by a Games-Howell multiple-group comparison test was used to compare differences between groups in animal experiments. P values < 0.05 were considered statistically significant.

Results

In vitro radiosensitizing effect of OBP-301 in human STS cells

To evaluate the radiosensitizing effect of OBP-301 in STS cells, we first analyzed the baseline sensitivity of four human STS cell lines (RD-ES, SK-ES-1, HT1080, and NMS-2) to ionizing radiation. The viability of RD-ES and SK-ES-1 (Ewing sarcoma) cells when irradiated at 2 Gy was decreased to approximately half that of non-irradiated cells, as measured by XTT assay (Fig 1A). In contrast, the viability of HT1080 (fibrosarcoma) and NMS-2 (MPNST) was reduced by less than 50% compared to the viability of non-irradiated cells, even up to 10 Gy (Fig 1A). These results indicate that RD-ES and SK-ES-1 cells are highly radiosensitive, whereas HT1080 and NMS-2 cells are moderately radiosensitive.

We next evaluated the combined effect of OBP-301 and ionizing radiation on viability. All four STS cell lines were irradiated 24 h after OBP-301 infection, and cell viability was assessed on day 4 after irradiation. The combination of OBP-301 and ionizing radiation decreased the viability of all STS cell lines more efficiently than single treatment (Fig 1B). Calculation of the combination index indicated a synergistic antitumor effect of combination therapy in all STS cell lines, although in moderately radiosensitive NMS-2 cells there was an antagonistic effect found with low doses of ionizing radiation and OBP-301 (Fig 1C). These results suggest that OBP-301 may act as a potent radiosensitizer in human STS cells.

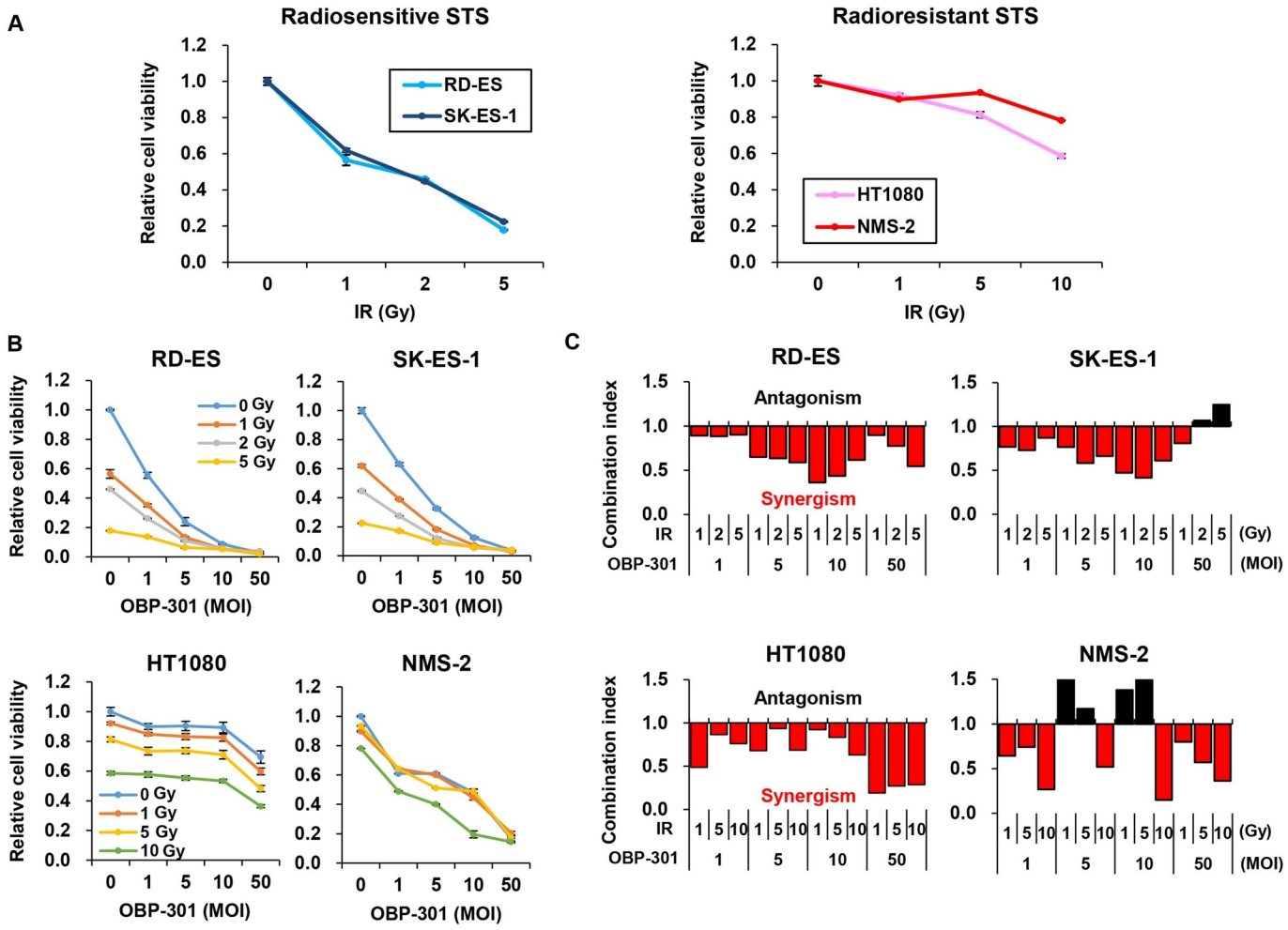

Fig 1. ***In vitro*** **radiosensitizing effect of OBP-301 on human soft tissue sarcoma cells. A**, Four human soft tissue sarcoma (STS) cell lines (RD-ES, SK-ES-1, HT1080, NMS-2) were irradiated at the indicated dose, and cell viability was assessed 4 days after irradiation using the XTT assay. RD-ES and SK-ES-1 cells are highly radiosensitive, whereas HT1080 and NMS-2 cells are moderately radiosensitive. Data are expressed as mean ± SD of independent experiments ($n = 5$). **B**, Cells were irradiated at the indicated doses 24 h after infection with OBP-301 at the indicated MOIs, and cell viability was assessed 4 days after irradiation. **C**, The combination index was calculated using CalcuSyn software. Synergism and antagonism were defined as interaction indices of < 1 and > 1, respectively.

https://doi.org/10.1371/journal.pone.0250643.g001

Suppression of anti-apoptotic MCL1 is involved in enhancing ionizing radiation-induced apoptosis by OBP-301

To investigate the underlying molecular mechanism in the OBP-301-mediated enhancement of radiotherapy, we analyzed the level of anti-apoptotic MCL1 expression in all STS cells. Interestingly, moderately radiosensitive HT1080 and NMS-2 cells exhibited high expression of MCL1 protein, whereas highly radiosensitive RD-ES and SK-ES-1 cells showed low expression of MCL1 protein (Fig 2A). These results suggest that the expression of MCL1 is associated with the radiosensitivity of STS cells.

We recently reported that OBP-301 enhances the cytotoxic effect of chemotherapeutic agents in human osteosarcoma cells by suppressing MCL1 expression through the activation of a transcription factor E2F1-microRNA pathway, resulting in the induction of apoptosis [17]. Therefore, we next assessed whether OBP-301 enhances ionizing radiation-induced apoptosis by suppressing MCL1 expression in highly radiosensitive SK-ES-1 and moderately

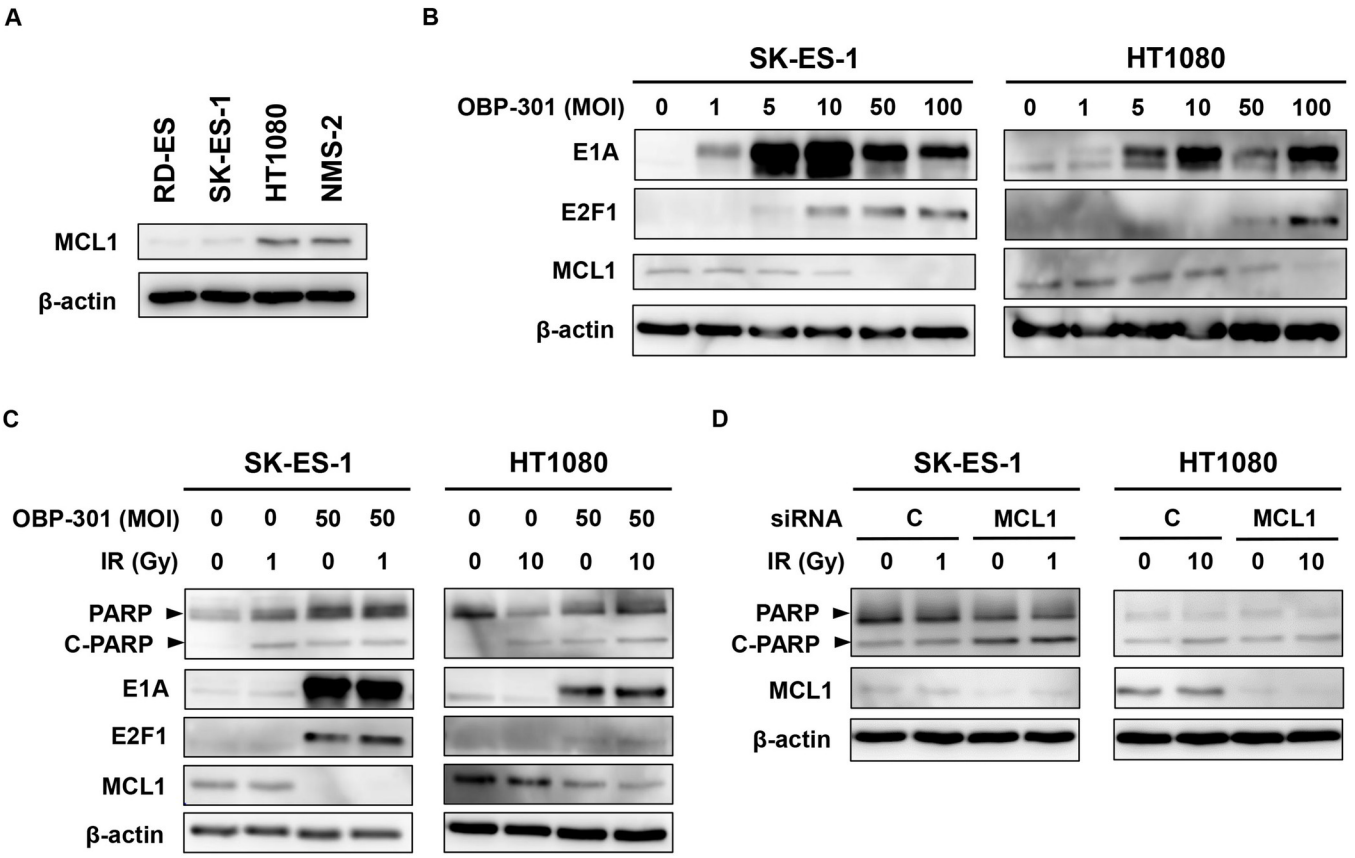

Fig 2. MCL1 suppression is involved in the OBP-301-mediated enhancement of apoptosis induced by ionizing radiation. A, Cell lysates were analyzed by Western blot for MCL1 expression. **B**, SK-ES-1 and HT1080 cells were infected with OBP-301 at the indicated MOIs for 72 h, and cell lysates were analyzed by Western blot for E1A, E2F1, and MCL1. **C**, SK-ES-1 and HT1080 cells were treated with OBP-301 and then irradiated (IR) at the indicated doses 24 h after infection, and cell lysates were subjected to Western blot for PARP, cleaved PARP (C-PARP), E1A, E2F1, and MCL1. **D**, SK-ES-1 and HT1080 cells were transfected with 10 nM MCL1 siRNA or control siRNA for 48 h, and subsequently irradiated at the indicated doses. Cell lysates were analyzed by Western blot for PARP, C-PARP, and MCL1. β-actin was assayed as a loading control.

https://doi.org/10.1371/journal.pone.0250643.g002

radiosensitive HT1080 cells. OBP-301 infection at high doses increased the expression of adenoviral E1A and E2F1, whereas MCL1 expression was decreased in SK-ES-1 and HT1080 cells (Fig 2B). The combination of OBP-301 and ionizing radiation induced apoptosis (PARP cleavage) in SK-ES-1 and HT1080 cells, which was associated with the upregulation of E2F1 and downregulation of MCL1 (Fig 2C). To further confirm the role of MCL1 suppression in radiation-induced apoptosis, we assessed the effect of MCL1 knockdown by RNA interference. MCL1 siRNA suppressed MCL1 expression and resulted in the enhancement of ionizing radiation-induced apoptosis in SK-ES-1 and HT1080 cells compared to control siRNA (Fig 2D). These results suggest that OBP-301 enhances ionizing radiation-mediated apoptosis induction via MCL1 suppression.

Enhancement of ionizing radiation-induced DNA damage by OBP-301

Therefore, we next investigated whether OBP-301 infection enhances ionizing radiation-induced accumulation of DNA damage by evaluating the expression of γH2AX in SK-ES-1 cells. Ionizing radiation, when combined with OBP-301 infection, increased γH2AX expression in SK-ES-1 cells 30 min after treatment. At 1 and 3 h after irradiation, the level of γH2AX expression remained elevated in OBP-301-infected cells. In contrast, in non-infected cells,

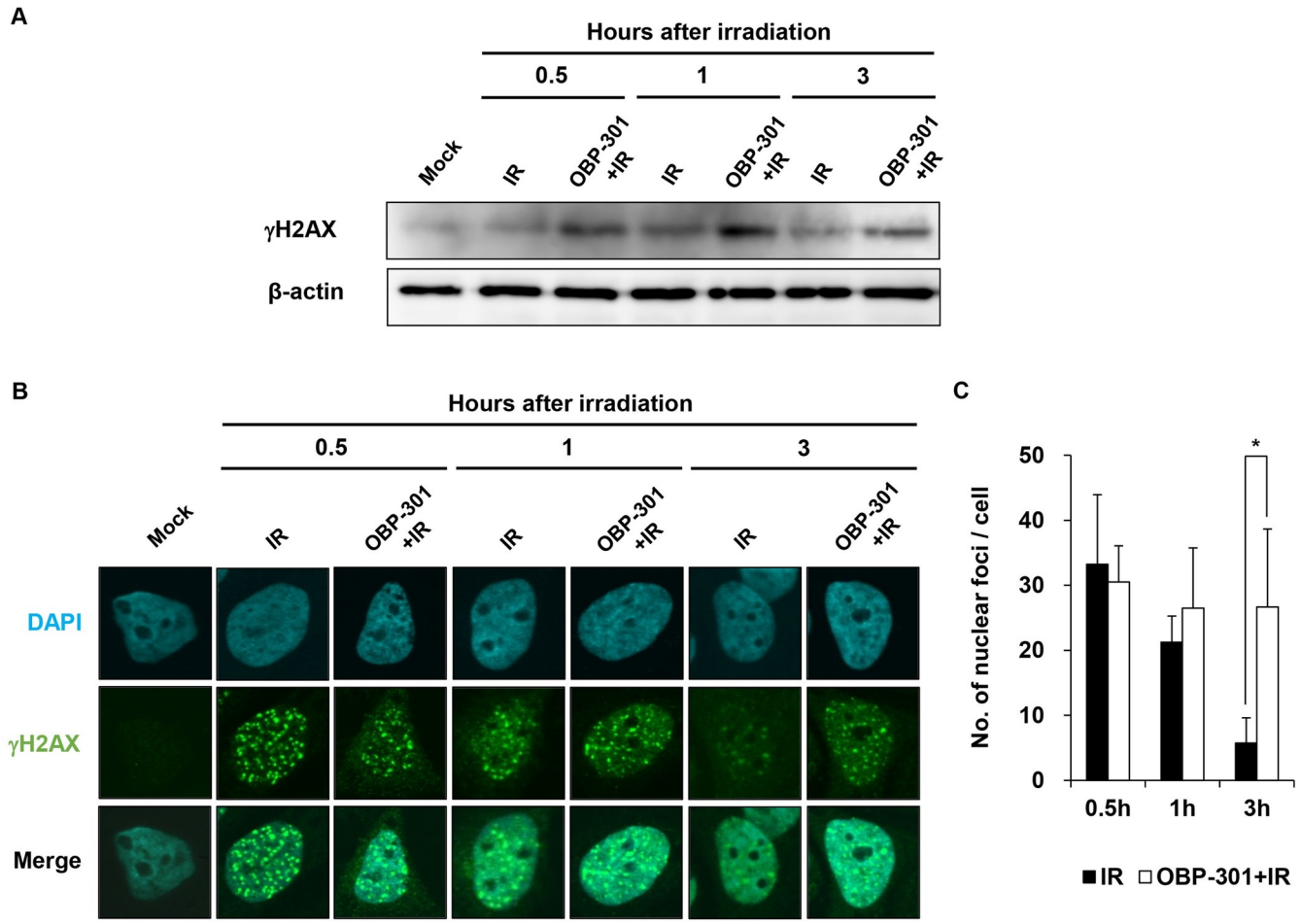

Fig 3. Enhancement of ionizing radiation-induced DNA damage by OBP-301. A, SK-ES-1 cells were infected with OBP-301 (10 MOI) and then irradiated at 1 Gy, 24 h after infection. Cells were harvested 0.5, 1, and 3 h after irradiation and analyzed by Western blot for γH2AX expression. **B**, SK-ES-1 cells were infected with OBP-301 (5 MOI) and then irradiated at 1 Gy, 24 h after infection. Cells were stained for γH2AX at 0.5, 1, and 3 h after irradiation and analyzed by confocal laser microscopy. **C**, The average number of γH2AX foci per cell. Data are expressed as mean ± SD of independent experiments ($n = 5$; *, $P < 0.05$).

https://doi.org/10.1371/journal.pone.0250643.g003

ionizing radiation increased γH2AX expression at 1 h, but the level gradually decreased following the repair of DNA damage (Fig 3A). To further evaluate the amount of DNA damage, we analyzed immunofluorescence staining of γH2AX using SK-ES-1 cells. There was no significant difference in the number of nuclear γH2AX foci between OBP-301-infected and non-infected cells at 30 min and 1 h following irradiation. However, at 3 h after irradiation, the number of nuclear γH2AX foci was significantly lower in non-infected cells compared to OBP-301-infected cells (Fig 3B and 3C). These results suggest that OBP-301 prolongs the accumulation of ionizing radiation-induced DNA damage.

Effect of combination therapy in subcutaneous STS tumor tissues

To confirm the radiosensitizing effect of OBP-301 in tumor tissues, we assessed the level of Ki67-positive (proliferation marker), TUNEL-positive (apoptosis marker), and γH2AX-positive staining (DNA damage marker) in subcutaneous xenograft tumors grown from highly radiosensitive SK-ES-1 and moderately radiosensitive HT1080 cells (Figs 4 and 5). Tumor-bearing mice were irradiated at 1 Gy (SK-ES-1) or 3 Gy (HT1080) after treatment with an

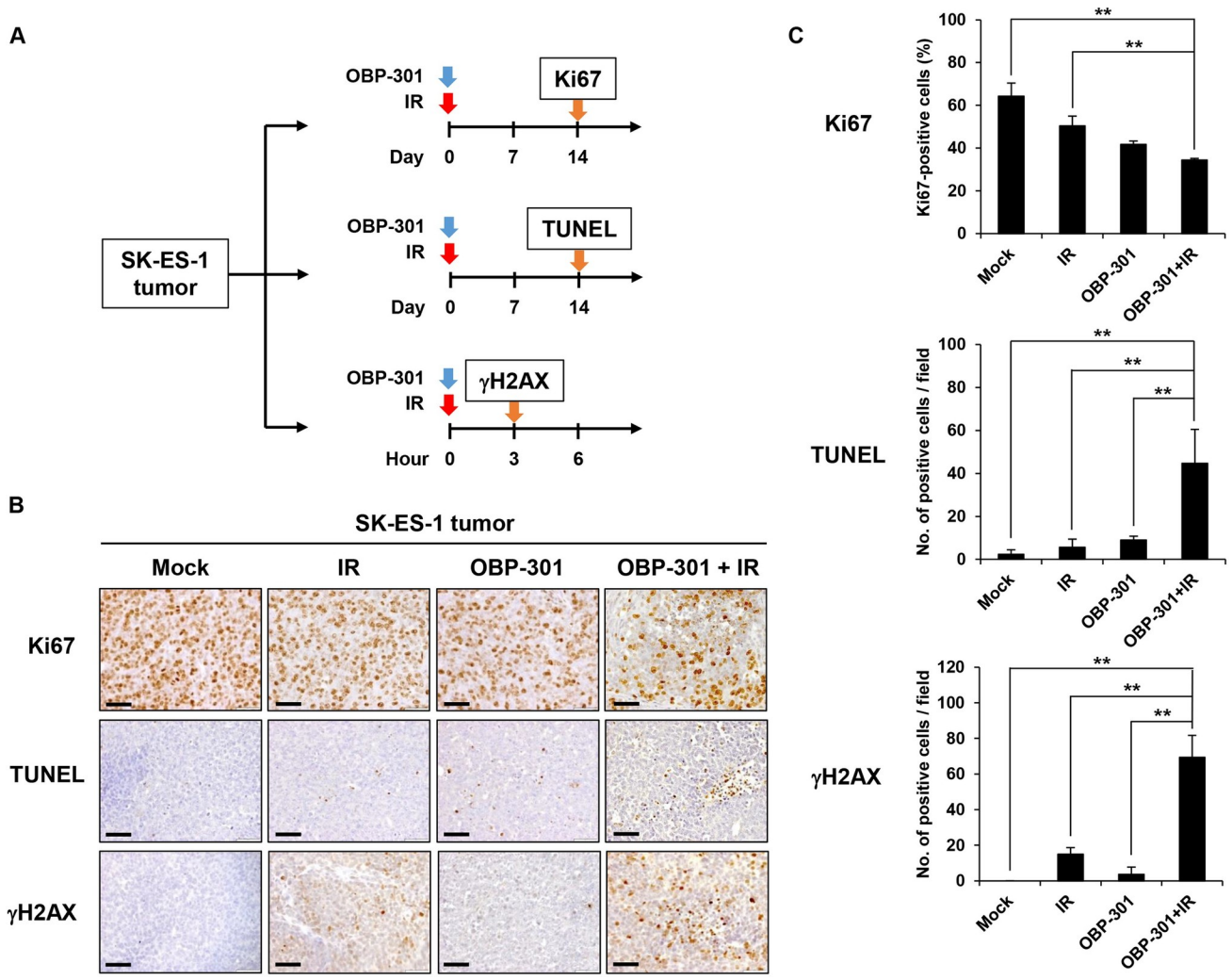

Fig 4. Suppression of proliferation and induction of apoptosis and DNA damage in subcutaneous SK-ES-1 xenograft tumors treated with OBP-301 and ionizing radiation. A, Scheme of treatment protocol used in conjunction with Ki67, TUNEL, and γH2AX assays. SK-ES-1 cells (5×10^6 cells/mouse) were subcutaneously inoculated into the right flanks of mice. Tumor-bearing mice were irradiated at 1 Gy after treatment with an intratumoral injection of OBP-301 (1×10^8 PFU/tumor). **B**, SK-ES-1 subcutaneous tumor sections were immunostained for Ki67, TUNEL, and γH2AX. Scale bar, 50 μm. **C**, The number of positive cells for Ki67, TUNEL, and γH2AX staining. Data are expressed as mean ± SD of independent experiments ($n = 3$ in each group; **, $P < 0.01$).

https://doi.org/10.1371/journal.pone.0250643.g004

intratumoral injection of OBP-301 (1×10^8 PFU/tumor). Subsequent immunohistochemical analysis demonstrated that the combination of OBP-301 and ionizing radiation significantly decreased the percentage of Ki67-positive proliferating cells compared to mock or single treatment in SK-ES-1 tumor tissues (Fig 4B and 4C). The number of TUNEL-positive cells was significantly increased in combination therapy-treated SK-ES-1 tumors compared with mock or monotherapy-treated tumors (Fig 4C). Moreover, combination therapy significantly increased the number of γH2AX-positive cells within SK-ES-1 tumor tissues (Fig 4C). Immunohistochemical analysis for moderately radiosensitive HT1080 tumors demonstrated similar findings, in that the percentage of Ki-67-positive cells was significantly decreased, and the number of TUNEL-positive and γH2AX-positive cells was significantly increased, in combination therapy-treated tumor tissues (Fig 5). These results suggest that the biological interaction between OBP-301 and ionizing radiation is induced in *in vivo* tumor tissues as well as *in vitro*.

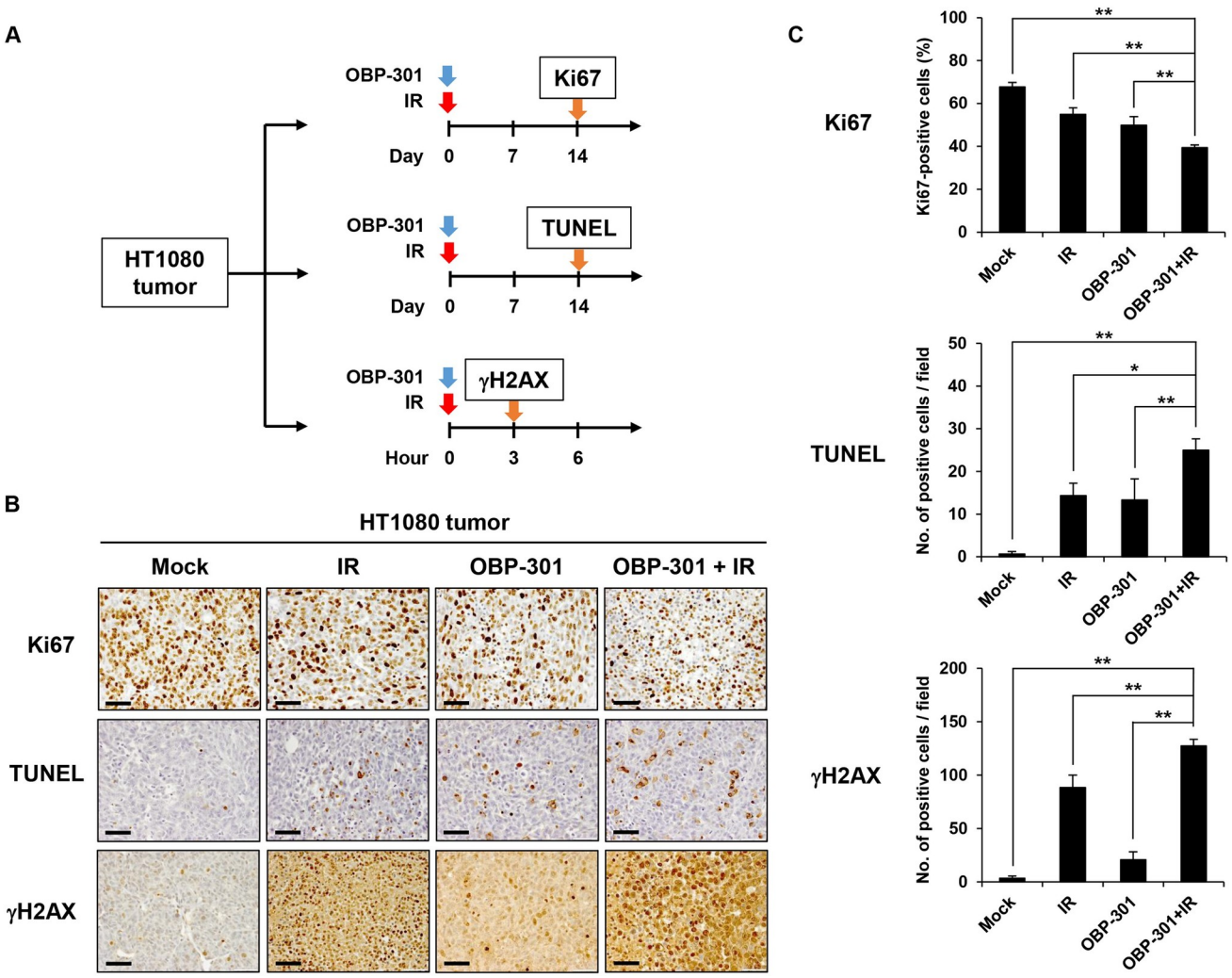

Fig 5. Suppression of proliferation and induction of apoptosis and DNA damage in subcutaneous HT1080 xenograft tumors treated with OBP-301 and ionizing radiation. A, Scheme of treatment protocol used in conjunction with Ki67, TUNEL, and γH2AX assays. HT1080 cells (3×10^6 cells/mouse) were subcutaneously inoculated into the right flanks of mice. Tumor-bearing mice were irradiated at 3 Gy after treatment with an intratumoral injection of OBP-301 (1×10^8 PFU/tumor). **B**, HT1080 subcutaneous tumor sections were immunostained for Ki67, TUNEL, and γH2AX. Scale bar, 50 μm. **C**, The number of positive cells for Ki67, TUNEL, and γH2AX. Data are expressed as mean ± SD of independent experiments ($n = 3$ in each group; *, $P < 0.05$; **, $P < 0.01$).

https://doi.org/10.1371/journal.pone.0250643.g005

Combination of OBP-301 and ionizing radiation inhibits the in vivo growth of STS tumors with different radiosensitivities

To assess the *in vivo* therapeutic efficacy of OBP-301 in combination with ionizing radiation, we again used the subcutaneous xenograft models for highly radiosensitive SK-ES-1 (Fig 6A) and moderately radiosensitive HT1080 cells (Fig 6B). Highly radiosensitive SK-ES-1 tumors were injected with OBP-301 (1×10^8 PFU/tumor) or PBS, and subsequently irradiated at 1 Gy every week for three cycles, with tumor growth observed for 28 days after the first treatment. The combination of OBP-301 and ionizing radiation showed a more profound antitumor effect in highly radiosensitive SK-ES-1 tumors compared with ionizing radiation alone (Fig 6A). Moderately radiosensitive HT1080 tumors were injected with OBP-301 (1×10^8 PFU/tumor) or PBS, and subsequently irradiated at 3 Gy every week for three cycles. Consistent

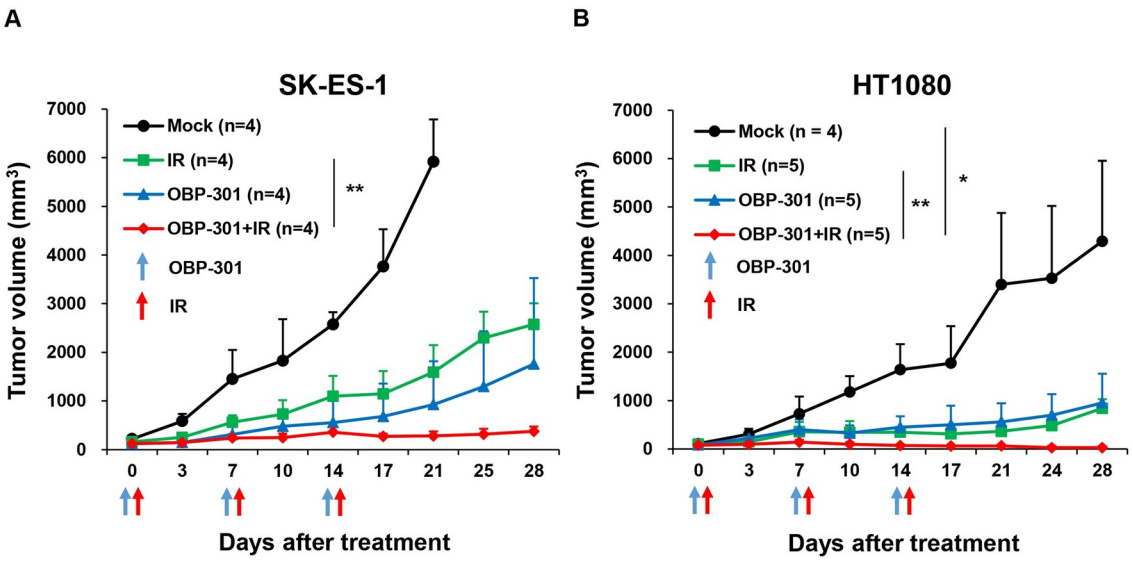

Fig 6. ***In vivo*** **antitumor effect of combination therapy with OBP-301 and ionizing radiation in the highly radiosensitive SK-ES-1 and moderately radiosensitive HT1080 xenograft tumor models. A** and **B**, SK-ES-1 cells (5×10^6 cells/mouse) or HT1080 cells (3×10^6 cells/mouse) were subcutaneously inoculated into the right flanks of mice. When tumors reached 5 to 7 mm in diameter, tumor-bearing mice were irradiated at 1 Gy (SK-ES-1) or 3 Gy (HT1080) after treatment with an intratumoral injection of OBP-301 (1×10^8 PFU/tumor) for three cycles every week (arrows indicate each treatment administration). The mock treatment group was sacrificed on day 21 in the SK-ES-1 and HT1080 tumor models, when tumor volumes reached approximately 4000 mm^3. Tumor growth is expressed as mean tumor volume ± SD of independent experiments (n = 4 to 5 in each group; *, $P < 0.05$; **, $P < 0.01$).

https://doi.org/10.1371/journal.pone.0250643.g006

with the findings from highly radiosensitive SK-ES-1 tumors, the combination of OBP-301 and ionizing radiation resulted in significant suppression of tumor growth compared with ionizing radiation alone (Fig 6B). However, there was no significant difference between groups treated with combination therapy and monotherapy with OBP-301 in these xenograft models (Fig 6A and 6B). There was no significant difference in the mean body weight of mice between the treatment groups (S7 Fig). These results suggest that combination therapy with OBP-301 and ionizing radiation efficiently inhibits the growth of STS tumors *in vivo*.

Discussion

The multidisciplinary approach to STS treatment involves surgery, radiotherapy, and chemotherapy. Although surgical resection and radiotherapy are the most frequent option for STS, resistance to radiotherapy contributes to tumor recurrence, metastasis, and poor prognosis [3,4]. Therefore, the enhancement of radiosensitivity is a critical aspect of improving clinical outcomes for STS patients, including minimizing the risk of secondary cancer by reducing the required dose of ionizing radiation. In this study, we demonstrated that combination therapy with OBP-301 and ionizing radiation has a synergistic antitumor effect in both highly radiosensitive and moderately radiosensitive STS cells. The profound antitumor effect of combination therapy was mainly due to OBP-301-mediated enhancement of ionizing radiation-induced apoptosis and DNA damage, via suppression of anti-apoptotic MCL1 expression. Several reports have suggested that MCL1 suppression with siRNA or small molecule inhibitors enhances sensitivity to ionizing radiation-induced apoptosis in human cancer cells, including melanoma [22], non-small cell lung cancer [23], and pancreatic cancer [24]. Thus, the combination of OBP-301 and ionizing radiation appears to be a promising antitumor strategy for improving the efficacy of radiotherapy in STS patients.

Our results demonstrated that moderately radiosensitive STS cells (HT1080 and NMS-2) have higher expression of MCL1 compared to highly radiosensitive STS cells (RD-ES and SK-ES-1), and suggested a role for MCL1 in the radiosensitivity of STS. We further demonstrated that MCL1 suppression by siRNA or OBP-301 enhanced ionizing radiation-induced apoptosis in STS cells. Similarly, it has been shown that MCL1 suppression with siRNA or antisense oligonucleotides enhances chemotherapy-induced apoptosis in human STS cells [25]. Thus, anti-apoptotic MCL1 may be a promising therapeutic target for improving sensitivity to both radiotherapy and chemotherapy in STS. Although our data supports that MCL1 is a key molecule involved in the radiosensitivity of STS, further experiments would be needed to confirm whether MCL1 suppression enhances radiation-induced apoptosis in STS cells.

Previous reports have suggested that oncolytic adenoviruses suppress MCL1 expression in infected cells [26,27], and the mechanism has been linked to adenoviral E1A accumulation [28]. Adenoviral E1A accumulation induces the activation of transcription factor E2F1 [29], which can contribute to MCL1 suppression [30,31]. These findings suggest that E1A-mediated E2F1 activation is critical for the downregulation of MCL1 expression by oncolytic adenovirus. Recently, we revealed that OBP-301 suppresses MCL1 expression in human osteosarcoma cells through E2F1-mediated upregulation of the MCL1-targeting non-coding microRNA miR-29 [17]. Recent reports have further suggested a role for miR-29 in improving the radiosensitivity of human cancers, including nasopharyngeal cancer [32] and lung cancer [33], via suppression of MCL1 expression. Ionizing radiation itself also suppresses MCL1 expression, by inducing miR-193a expression, resulting in the induction of apoptosis [34]. Therefore, the activation of an MCL1-targeting miRNA signaling pathway may be implicated in the combination therapy-mediated MCL1 suppression that we have observed in the present study.

In the present study, OBP-301 significantly enhanced the level of γH2AX in irradiated tumor cells both *in vitro* and *in vivo*, suggesting that OBP-301 has the potential to enhance ionizing radiation-induced DNA damage and thus the sensitivity to ionizing radiation. We previously reported that OBP-301 inhibits the DNA damage repair pathway via adenoviral E1B-dependent degradation of the MRN complex, which consists of Mre11, Rad50, and NBS1 proteins [15]. Indeed, an accumulation of recent evidence has suggested that oncolytic adenovirus inhibits DNA damage repair pathways via direct interaction between adenoviral proteins and DNA damage response-related factors [35]. On the other hand, previous work has demonstrated that MCL1 is associated with γH2AX and NBS1 following chemotherapy-induced DNA damage in mouse embryo fibroblasts [36]. Mattoo and colleagues have shown that knockdown of MCL1 by siRNA in human cancer cells, including osteosarcoma, increases γH2AX levels after irradiation via impairment of the homologous recombination pathway [37]. Thus, adenoviral protein accumulation and MCL1 reduction may be cooperatively involved in the OBP-301-mediated inhibition of DNA damage repair.

HT1080 tumors were radiosensitive as similar with SK-ES-1 tumors. These findings suggest that HT1080 tumors are not suitable to mimic the radioresistant STS tumors. Resistance to radiotherapy is thought to be associated with the existence of cancer stem-like cells [38]. The dormancy of such cells is a critical factor for the radioresistance of tumors, because radiotherapy targets proliferating cancer cells by inducing DNA damage-related cell cycle arrest. Several reports have suggested that a CD133-positive subpopulation of radioresistant HT1080 cells exhibit cancer stem-like characteristics [39,40]. CD133-positive subpopulations have similarly been associated with the radioresistance of brain tumor [41], liver cancer [42], and lung cancer [43]. We previously demonstrated that OBP-301 efficiently kills radioresistant CD133-positive cells, as well as radiosensitive CD133-negative cells, in human gastric cancer [44]. Therefore, HT1080 tumors derived from radioresistant CD133-positive cells may be more suitable model

to investigate the therapeutic potential of combination therapy with OBP-301 and ionizing radiation.

In conclusion, we have demonstrated that combination therapy with OBP-301 and ionizing radiation exerts a synergistic antitumor effect in STS cells. OBP-301 promoted ionizing radiation-induced apoptosis through suppression of anti-apoptotic MCL1 expression and enhancement of DNA damage. Furthermore, combination therapy showed a more profound antitumor effect compared to monotherapy in highly and moderately radiosensitive STS xenograft tumors. Thus, combination therapy with OBP-301 and ionizing radiation offers a promising antitumor strategy to improve the clinical outcome of radiotherapy-treated STS patients. Further clinical studies are warranted to investigate the tolerability and efficacy of this combination therapy for the treatment of STS patients.

Supporting information

S1 Fig. Full images of Fig 2A.
(PDF)

S2 Fig. Full images of Fig 2B (SK-ES-1).
(PDF)

S3 Fig. Full images of Fig 2B (HT1080).
(PDF)

S4 Fig. Full images of Fig 2C (SK-ES-1).
(PDF)

S5 Fig. Full images of Fig 2C (HT1080).
(PDF)

S6 Fig. Full images of Fig 2D.
(PDF)

S7 Fig. Chronological change in the body weight of xenograft tumor-bearing mice treated with OBP-301 and/or ionizing radiation.
(PDF)

Acknowledgments

We thank Dr. Hiroyuki Kawashima (Niigata University) for providing NMS-2 cells, and Ms. Tomoko Sueishi and Mr. Takeshi Ieda for their excellent technical support.

Author Contributions

Conceptualization: Hiroshi Tazawa, Toshifumi Ozaki, Toshiyoshi Fujiwara.

Data curation: Toshinori Omori, Yasuaki Yamakawa, Shuhei Osaki, Joe Hasei, Kazuhisa Sugiu, Tadashi Komatsubara, Tomohiro Fujiwara, Aki Yoshida.

Formal analysis: Toshinori Omori, Hiroshi Tazawa, Yasuaki Yamakawa, Shuhei Osaki.

Investigation: Toshinori Omori.

Methodology: Toshinori Omori, Hiroshi Tazawa, Yasuaki Yamakawa, Shuhei Osaki.

Resources: Yasuo Urata.

Supervision: Hiroshi Tazawa, Toshiyuki Kunisada, Shunsuke Kagawa, Toshifumi Ozaki, Toshiyoshi Fujiwara.

Writing – original draft: Toshinori Omori, Hiroshi Tazawa, Toshiyoshi Fujiwara.

Writing – review & editing: Hiroshi Tazawa, Toshiyoshi Fujiwara.

References

1. Jemal A, Siegel R, Xu J, Ward E. Cancer statistics, 2010. CA Cancer J Clin. 2010; 60(5):277–300. https://doi.org/10.3322/caac.20073 PMID: 20610543
2. Pisters PW, O'Sullivan B, Maki RG. Evidence-based recommendations for local therapy for soft tissue sarcomas. J Clin Oncol. 2007; 25(8):1003–8. https://doi.org/10.1200/JCO.2006.09.8525 PMID: 17350950
3. Gamboa AC, Gronchi A, Cardona K. Soft-tissue sarcoma in adults: An update on the current state of histiotype-specific management in an era of personalized medicine. CA Cancer J Clin. 2020; 70 (3):200–29. https://doi.org/10.3322/caac.21605 PMID: 32275330
4. Begg AC, Stewart FA, Vens C. Strategies to improve radiotherapy with targeted drugs. Nat Rev Cancer. 2011; 11(4):239–53. https://doi.org/10.1038/nrc3007 PMID: 21430696
5. Gilbert NF, Cannon CP, Lin PP, Lewis VO. Soft-tissue sarcoma. J Am Acad Orthop Surg. 2009; 17 (1):40–7. https://doi.org/10.5435/00124635-200901000-00006 PMID: 19136426
6. Davis AM, O'Sullivan B, Turcotte R, Bell R, Catton C, Chabot P, et al. Late radiation morbidity following randomization to preoperative versus postoperative radiotherapy in extremity soft tissue sarcoma. Radiother Oncol. 2005; 75(1):48–53. https://doi.org/10.1016/j.radonc.2004.12.020 PMID: 15948265
7. Tang Z, Zeng Q, Li Y, Zhang X, Ma J, Suto MJ, et al. Development of a radiosensitivity gene signature for patients with soft tissue sarcoma. Oncotarget. 2017; 8(16):27428–39. https://doi.org/10.18632/oncotarget.16194 PMID: 28404969
8. Thway K. Pathology of soft tissue sarcomas. Clin Oncol (R Coll Radiol). 2009; 21(9):695–705.
9. Kuo LJ, Yang LX. Gamma-H2AX—a novel biomarker for DNA double-strand breaks. In Vivo. 2008; 22 (3):305–9. PMID: 18610740
10. Banath JP, Macphail SH, Olive PL. Radiation sensitivity, H2AX phosphorylation, and kinetics of repair of DNA strand breaks in irradiated cervical cancer cell lines. Cancer Res. 2004; 64(19):7144–9. https://doi.org/10.1158/0008-5472.CAN-04-1433 PMID: 15466212
11. Beroukhim R, Mermel CH, Porter D, Wei G, Raychaudhuri S, Donovan J, et al. The landscape of somatic copy-number alteration across human cancers. Nature. 2010; 463(7283):899–905. https://doi.org/10.1038/nature08822 PMID: 20164920
12. Kawashima T, Kagawa S, Kobayashi N, Shirakiya Y, Umeoka T, Teraishi F, et al. Telomerase-specific replication-selective virotherapy for human cancer. Clin Cancer Res. 2004; 10(1 Pt 1):285–92. https://doi.org/10.1158/1078-0432.ccr-1075-3 PMID: 14734481
13. Hashimoto Y, Watanabe Y, Shirakiya Y, Uno F, Kagawa S, Kawamura H, et al. Establishment of biological and pharmacokinetic assays of telomerase-specific replication-selective adenovirus. Cancer Sci. 2008; 99(2):385–90. https://doi.org/10.1111/j.1349-7006.2007.00665.x PMID: 18201270
14. Sasaki T, Tazawa H, Hasei J, Kunisada T, Yoshida A, Hashimoto Y, et al. Preclinical evaluation of telomerase-specific oncolytic virotherapy for human bone and soft tissue sarcomas. Clin Cancer Res. 2011; 17(7):1828–38. https://doi.org/10.1158/1078-0432.CCR-10-2066 PMID: 21325287
15. Kuroda S, Fujiwara T, Shirakawa Y, Yamasaki Y, Yano S, Uno F, et al. Telomerase-dependent oncolytic adenovirus sensitizes human cancer cells to ionizing radiation via inhibition of DNA repair machinery. Cancer Res. 2010; 70(22):9339–48. https://doi.org/10.1158/0008-5472.CAN-10-2333 PMID: 21045143
16. Liu D, Kojima T, Ouchi M, Kuroda S, Watanabe Y, Hashimoto Y, et al. Preclinical evaluation of synergistic effect of telomerase-specific oncolytic virotherapy and gemcitabine for human lung cancer. Mol Cancer Ther. 2009; 8(4):980–7. https://doi.org/10.1158/1535-7163.MCT-08-0901 PMID: 19372571
17. Osaki S, Tazawa H, Hasei J, Yamakawa Y, Omori T, Sugiu K, et al. Ablation of MCL1 expression by virally induced microRNA-29 reverses chemoresistance in human osteosarcomas. Sci Rep. 2016; 6:28953. https://doi.org/10.1038/srep28953 PMID: 27356624
18. Yamakawa Y, Tazawa H, Hasei J, Osaki S, Omori T, Sugiu K, et al. Role of zoledronic acid in oncolytic virotherapy: Promotion of antitumor effect and prevention of bone destruction. Cancer Sci. 2017; 108 (9):1870–80. https://doi.org/10.1111/cas.13316 PMID: 28685948

19. Nemunaitis J, Tong AW, Nemunaitis M, Senzer N, Phadke AP, Bedell C, et al. A phase I study of telomerase-specific replication competent oncolytic adenovirus (telomelysin) for various solid tumors. Mol Ther. 2010; 18(2):429–34. https://doi.org/10.1038/mt.2009.262 PMID: 19935775

20. Imaizumi S, Motoyama T, Ogose A, Hotta T, Takahashi HE. Characterization and chemosensitivity of two human malignant peripheral nerve sheath tumour cell lines derived from a patient with neurofibromatosis type 1. Virchows Archiv-an International Journal of Pathology. 1998; 433(5):435–41. https://doi.org/10.1007/s004280050271 PMID: 9849858

21. Chou TC. Theoretical basis, experimental design, and computerized simulation of synergism and antagonism in drug combination studies. Pharmacol Rev. 2006; 58(3):621–81. https://doi.org/10.1124/pr.58.3.10 PMID: 16968952

22. Skvara H, Thallinger C, Wacheck V, Monia BP, Pehamberger H, Jansen B, et al. Mcl-1 blocks radiation-induced apoptosis and inhibits clonogenic cell death. Anticancer Res. 2005; 25(4):2697–703. PMID: 16080514

23. Song L, Coppola D, Livingston S, Cress D, Haura EB. Mcl-1 regulates survival and sensitivity to diverse apoptotic stimuli in human non-small cell lung cancer cells. Cancer Biol Ther. 2005; 4(3):267–76. https://doi.org/10.4161/cbt.4.3.1496 PMID: 15753661

24. Wei D, Zhang Q, Schreiber JS, Parsels LA, Abulwerdi FA, Kausar T, et al. Targeting mcl-1 for radiosensitization of pancreatic cancers. Transl Oncol. 2015; 8(1):47–54. https://doi.org/10.1016/j.tranon.2014.12.004 PMID: 25749177

25. Thallinger C, Wolschek MF, Maierhofer H, Skvara H, Pehamberger H, Monia BP, et al. Mcl-1 is a novel therapeutic target for human sarcoma: synergistic inhibition of human sarcoma xenotransplants by a combination of Mcl-1 antisense Oligonucleotides with low-dose cyclophosphamide. Clinical Cancer Research. 2004; 10(12):4185–91. https://doi.org/10.1158/1078-0432.CCR-03-0774 PMID: 15217956

26. Wirth T, Kuhnel F, Fleischmann-Mundt B, Woller N, Djojosubroto M, Rudolph KL, et al. Telomerase-dependent virotherapy overcomes resistance of hepatocellular carcinomas against chemotherapy and tumor necrosis factor-related apoptosis-inducing ligand by elimination of Mcl-1. Cancer Res. 2005; 65(16):7393–402. https://doi.org/10.1158/0008-5472.CAN-04-3664 PMID: 16103092

27. You L, Wang Y, Jin Y, Qian W. Downregulation of Mcl-1 synergizes the apoptotic response to combined treatment with cisplatin and a novel fiber chimeric oncolytic adenovirus. Oncol Rep. 2012; 27(4):971–8. https://doi.org/10.3892/or.2012.1636 PMID: 22266706

28. Cuconati A, Mukherjee C, Perez D, White E. DNA damage response and MCL-1 destruction initiate apoptosis in adenovirus-infected cells. Genes Dev. 2003; 17(23):2922–32. https://doi.org/10.1101/gad.1156903 PMID: 14633975

29. Bagchi S, Raychaudhuri P, Nevins JR. Adenovirus E1A proteins can dissociate heteromeric complexes involving the E2F transcription factor: a novel mechanism for E1A trans-activation. Cell. 1990; 62(4):659–69. https://doi.org/10.1016/0092-8674(90)90112-r PMID: 2143697

30. Croxton R, Ma Y, Song L, Haura EB, Cress WD. Direct repression of the Mcl-1 promoter by E2F1. Oncogene. 2002; 21(9):1359–69. https://doi.org/10.1038/sj.onc.1205157 PMID: 11857079

31. Ma Y, Croxton R, Moorer RL Jr., Cress WD. Identification of novel E2F1-regulated genes by microarray. Arch Biochem Biophys. 2002; 399(2):212–24. https://doi.org/10.1006/abbi.2002.2761 PMID: 11888208

32. Zhang JX, Qian D, Wang FW, Liao DZ, Wei JH, Tong ZT, et al. MicroRNA-29c enhances the sensitivities of human nasopharyngeal carcinoma to cisplatin-based chemotherapy and radiotherapy. Cancer Lett. 2013; 329(1):91–8. https://doi.org/10.1016/j.canlet.2012.10.033 PMID: 23142283

33. Arechaga-Ocampo E, Lopez-Camarillo C, Villegas-Sepulveda N, Gonzalez-De la Rosa CH, Perez-Anorve IX, Roldan-Perez R, et al. Tumor suppressor miR-29c regulates radioresistance in lung cancer cells. Tumour Biol. 2017; 39(3):1010428317695010. https://doi.org/10.1177/1010428317695010 PMID: 28345453

34. Kwon JE, Kim BY, Kwak SY, Bae IH, Han YH. Ionizing radiation-inducible microRNA miR-193a-3p induces apoptosis by directly targeting Mcl-1. Apoptosis. 2013; 18(7):896–909. https://doi.org/10.1007/s10495-013-0841-7 PMID: 23546867

35. O'Cathail SM, Pokrovska TD, Maughan TS, Fisher KD, Seymour LW, Hawkins MA. Combining Oncolytic Adenovirus with Radiation-A Paradigm for the Future of Radiosensitization. Front Oncol. 2017; 7:153. https://doi.org/10.3389/fonc.2017.00153 PMID: 28791251

36. Jamil S, Stoica C, Hackett TL, Duronio V. MCL-1 localizes to sites of DNA damage and regulates DNA damage response. Cell Cycle. 2010; 9(14):2843–55. https://doi.org/10.4161/cc.9.14.12354 PMID: 20647761

37. Mattoo AR, Pandita RK, Chakraborty S, Charaka V, Mujoo K, Hunt CR, et al. MCL-1 Depletion Impairs DNA Double-Strand Break Repair and Reinitiation of Stalled DNA Replication Forks. Mol Cell Biol. 2017; 37(3). https://doi.org/10.1128/MCB.00535-16 PMID: 27821478

38. Butof R, Dubrovska A, Baumann M. Clinical perspectives of cancer stem cell research in radiation oncology. Radiother Oncol. 2013; 108(3):388–96. https://doi.org/10.1016/j.radonc.2013.06.002 PMID: 23830466

39. Liu WD, Zhang T, Wang CL, Meng HM, Song YW, Zhao Z, et al. Sphere-forming tumor cells possess stem-like properties in human fibrosarcoma primary tumors and cell lines. Oncol Lett. 2012; 4(6):1315–20. https://doi.org/10.3892/ol.2012.940 PMID: 23205129

40. Feng BH, Liu AG, Gu WG, Deng L, Cheng XG, Tong TJ, et al. CD133+ subpopulation of the HT1080 human fibrosarcoma cell line exhibits cancer stem-like characteristics. Oncol Rep. 2013; 30(2):815–23. https://doi.org/10.3892/or.2013.2486 PMID: 23708735

41. Bao S, Wu Q, McLendon RE, Hao Y, Shi Q, Hjelmeland AB, et al. Glioma stem cells promote radioresistance by preferential activation of the DNA damage response. Nature. 2006; 444(7120):756–60. https://doi.org/10.1038/nature05236 PMID: 17051156

42. Piao LS, Hur W, Kim TK, Hong SW, Kim SW, Choi JE, et al. CD133+ liver cancer stem cells modulate radioresistance in human hepatocellular carcinoma. Cancer Lett. 2012; 315(2):129–37. https://doi.org/10.1016/j.canlet.2011.10.012 PMID: 22079466

43. Desai A, Webb B, Gerson SL. CD133+ cells contribute to radioresistance via altered regulation of DNA repair genes in human lung cancer cells. Radiother Oncol. 2014; 110(3):538–45. https://doi.org/10.1016/j.radonc.2013.10.040 PMID: 24440048

44. Yano S, Tazawa H, Hashimoto Y, Shirakawa Y, Kuroda S, Nishizaki M, et al. A genetically engineered oncolytic adenovirus decoys and lethally traps quiescent cancer stem-like cells in S/G2/M phases. Clin Cancer Res. 2013; 19(23):6495–505. https://doi.org/10.1158/1078-0432.CCR-13-0742 PMID: 24081978